

Overview and Classification of Some Regularization Techniques for the Gauss-Newton Inversion Method Applied to Inverse Scattering Problems

Puyan Mojabi and Joe LoVetri, *Senior Member, IEEE*

Abstract—Different regularization techniques used in conjunction with the Gauss-Newton inversion method for electromagnetic inverse scattering problems are studied and classified into two main categories. The first category attempts to regularize the quadratic form of the nonlinear data misfit cost-functional at different iterations of the Gauss-Newton inversion method. This can be accomplished by utilizing penalty methods or projection methods. The second category tries to regularize the nonlinear data misfit cost-functional before applying the Gauss-Newton inversion method. This type of regularization may be applied via additive, multiplicative or additive-multiplicative terms. We show that these two regularization strategies can be viewed from a single consistent framework.

Index Terms—Inverse scattering, regularization.

I. INTRODUCTION

IN electromagnetic inverse scattering, one attempts to reconstruct the complex permittivity of the domain of interest using scattering measurements collected outside this domain. There are many applications for the inverse scattering problem, including industrial non-destructive testing [1], [2], geophysical surveys [3], [4], through-wall imaging [5] and biomedical imaging [6]–[8]. The inverse scattering problem is nonlinear and ill-posed. The nonlinearity of the problem is handled by utilizing different optimization algorithms such as the Gauss-Newton [3], [6], [9]–[18], quasi-Newton [19], conjugate gradient [20], [21], modified gradient [8], [22], [23], and global optimization techniques [24], [25]. The ill-posedness is treated via regularization. The general approach for regularizing an ill-posed problem is to set an appropriate constraint (or constraints) on the solution; e.g., limiting some (semi)norm of the solution or enforcing the solution to lie in an appropriate subspace. Different regularization methods usually require determining one or more regularization parameters which weight the regularization.

In this paper, we overview some regularization strategies which have been used with the Gauss-Newton Inversion (GNI) method for the electromagnetic inverse scattering problem. These strategies are classified into two main categories based

on the type of the cost-functional to be minimized. We show that these regularization strategies can all be viewed from a similar framework.

II. PROBLEM STATEMENT

Consider a bounded domain of interest \mathcal{D} , with an unknown complex relative permittivity $\epsilon_r(\mathbf{q})$, $\mathbf{q} \in \mathcal{D}$, which is immersed in a known background medium with complex relative permittivity ϵ_b . The electric contrast, defined as

$$\chi(\mathbf{q}) = \frac{\epsilon_r(\mathbf{q}) - \epsilon_b}{\epsilon_b} \quad (1)$$

is to be found using the measured electric field data on a measurement domain \mathcal{S} outside \mathcal{D} . Denoting $E^{\text{meas}}(\mathbf{p})$ as the measured scattered field on \mathcal{S} and $E^{\text{scat}}(\mathbf{p}, \chi(\mathbf{q}))$ as the simulated scattered field on \mathcal{S} due to a predicted contrast $\chi(\mathbf{q})$, the inverse scattering problem may then be formulated as the minimization over $\chi(\mathbf{q})$ of the data misfit cost-functional

$$\mathcal{F}^{\mathcal{L}\mathcal{S}}(\chi(\mathbf{q})) = \frac{1}{\mathcal{N}^{\mathcal{L}\mathcal{S}}} \|E^{\text{scat}}(\mathbf{p}, \chi(\mathbf{q})) - E^{\text{meas}}(\mathbf{p})\|_{\mathcal{S}}^2 \quad (2)$$

where $\mathbf{p} \in \mathcal{S}$ and $\|\cdot\|_{\mathcal{S}}$ denotes the L_2 -norm on functions defined on \mathcal{S} . The normalization constant $\mathcal{N}^{\mathcal{L}\mathcal{S}}$ is chosen to be $\|E^{\text{meas}}(\mathbf{p})\|_{\mathcal{S}}^2$. Denoting the wavenumber of the background medium as k_b and, for simplicity of notation, assuming the 2D Transverse Magnetic (TM) formulation, the simulated scattered field on \mathcal{S} due to the contrast $\chi(\mathbf{q})$ can be written as

$$E^{\text{scat}}(\mathbf{p}, \chi(\mathbf{q})) = k_b^2 \int_{\mathcal{D}} g(\mathbf{p}, \mathbf{q}) E(\mathbf{q}) \chi(\mathbf{q}) dv(\mathbf{q}) \quad (3)$$

where $E(\mathbf{q})$ represents the total field inside \mathcal{D} and $g(\mathbf{p}, \mathbf{q})$ is the appropriate Green's function for the problem. The total field $E(\mathbf{q})$ inside \mathcal{D} is related to the contrast $\chi(\mathbf{q})$ via the so-called domain equation

$$E(\mathbf{q}) = E^{\text{inc}}(\mathbf{q}) + k_b^2 \int_{\mathcal{D}} g(\mathbf{q}, \mathbf{q}') E(\mathbf{q}') \chi(\mathbf{q}') dv(\mathbf{q}') \quad (4)$$

where $E^{\text{inc}}(\mathbf{q})$ is the incident electric field inside the domain of interest \mathcal{D} which is assumed to be known. As can be seen from (3) and (4), the scattered field on the measurement domain is a nonlinear function with respect to the contrast $\chi(\mathbf{q})$; thus, making $\mathcal{F}^{\mathcal{L}\mathcal{S}}$ a nonlinear cost-functional. In this paper, we use

Manuscript received December 03, 2008; revised February 11, 2009. First published July 10, 2009; current version published September 02, 2009. This work was supported in part by the Natural Sciences and Engineering Research Council, in part by MITACS, and in part by CancerCare Manitoba.

The authors are with the Department of Electrical and Computer Engineering, University of Manitoba, Winnipeg, MB R3T5V6, Canada (e-mail: pmojabi@ee.umanitoba.ca).

Digital Object Identifier 10.1109/TAP.2009.2027161

the GNI method to deal with the nonlinearity of the problem. Note that the 2D TM formulation is utilized for simplicity of notation but the main result of the paper, i.e. the consistent framework in which to represent the different regularization schemes presented in Section V, is applicable to any other integral equation formulation of the inverse scattering problem, including vector scattering formulations based on the Green's dyadic.

Throughout this paper, we assume that the contrast $\chi(\mathbf{q})$ is discretized into a complex vector $\chi \in \mathbb{C}^N$ where N is the number of discretized elements in \mathcal{D} . We also assume that there is a finite number of measurements on \mathcal{S} . We, therefore, represent $E^{\text{meas}}(\mathbf{p})$ and $E^{\text{scat}}(\mathbf{p})$ as two complex vectors $E^{\text{meas}} \in \mathbb{C}^M$ and $E^{\text{scat}} \in \mathbb{C}^M$ where M is the number of measurements on \mathcal{S} .

III. THE GAUSS-NEWTON INVERSION METHOD

The Gauss-Newton inversion method is based on the Gauss-Newton optimization [26] where the nonlinear cost-functional is approximated with a quadratic form corresponding to the current iteration. The stationary point of the quadratic model is then chosen as the next iterate. Herein, the cost-functional to be minimized, say $\mathcal{F}(\chi)$, is either the data misfit $\mathcal{F}^{\mathcal{LS}}(\chi)$ or an augmented form thereof.

For the cost-functional $\mathcal{F}(\chi)$, we take the complex vector χ and its complex conjugate χ^* as two independent variables over which to perform the minimization. It is shown, [27], [28], that this procedure is equivalent with minimizing $\mathcal{F}(\chi)$ over the vectors χ_R and χ_I , the real and imaginary parts of the complex vector χ . Therefore, the Newton correction $\Delta\chi$ can be found by solving

$$\mathbf{H} \begin{pmatrix} \Delta\chi \\ \Delta\chi^* \end{pmatrix} = -g \quad (5)$$

where \mathbf{H} and g are the Hessian and gradient of $\mathcal{F}(\chi)$ respectively. These are defined as

$$\mathbf{H} = \begin{pmatrix} \frac{\partial^2 \mathcal{F}}{\partial \chi \partial \chi} & \frac{\partial^2 \mathcal{F}}{\partial \chi \partial \chi^*} \\ \frac{\partial^2 \mathcal{F}}{\partial \chi^* \partial \chi} & \frac{\partial^2 \mathcal{F}}{\partial \chi^* \partial \chi^*} \end{pmatrix} \in \mathbb{C}^{2N \times 2N} \quad (6)$$

$$g = \begin{pmatrix} \frac{\partial \mathcal{F}}{\partial \chi} \\ \frac{\partial \mathcal{F}}{\partial \chi^*} \end{pmatrix} \in \mathbb{C}^{2N}. \quad (7)$$

In the GNI method, the derivatives $\partial^2 \mathcal{F} / \partial \chi \partial \chi$ and $\partial^2 \mathcal{F} / \partial \chi^* \partial \chi^*$ are ignored to avoid their computational costs. Therefore, the Gauss-Newton (GN) correction at the n^{th} iteration may be found by solving

$$\partial^2 \mathcal{F} / \partial \chi^* \partial \chi |_{\chi=\chi_n} \Delta\chi_n = -\partial \mathcal{F} / \partial \chi^* |_{\chi=\chi_n}. \quad (8)$$

Having found the GN correction, the contrast at the n^{th} iteration of the GNI algorithm is updated as

$$\chi_{n+1} = \chi_n + \nu_n \Delta\chi_n \quad (9)$$

where ν_n is an appropriate step-length chosen to enforce the error reduction of the cost-functional. Depending on the choice

of the cost-functional $\mathcal{F}(\chi)$, (8) may become ill-posed or well-posed. Treating the ill-posedness via regularization is discussed in the next section.

If $\mathcal{F}^{\mathcal{LS}}$ is taken as the cost-functional to be minimized, the derivatives in (8) can be written as

$$\partial \mathcal{F}^{\mathcal{LS}} / \partial \chi^* |_{\chi=\chi_n} = -\frac{1}{\mathcal{N}^{\mathcal{LS}}} \mathbf{J}_n^H d_n \quad (10)$$

$$\partial^2 \mathcal{F}^{\mathcal{LS}} / \partial \chi^* \partial \chi |_{\chi=\chi_n} = \frac{1}{\mathcal{N}^{\mathcal{LS}}} \mathbf{J}_n^H \mathbf{J}_n \quad (11)$$

where the superscript ' H ' denotes the Hermitian operator. The vector $d_n \in \mathbb{C}^M$ is the discrepancy between the measured data and the simulated data corresponding to χ_n ; i.e., $d_n = E^{\text{meas}} - E_n^{\text{scat}}$. The Jacobian matrix $\mathbf{J}_n \in \mathbb{C}^{M \times N}$ contains the derivative of E_n^{scat} with respect to χ evaluated at χ_n . The analytic expression for \mathbf{J}_n , or an approximation thereof, which may be derived using an adjoint formulation [29], can be found in different publications such as [3], [16], [19].

IV. REGULARIZATION

Two general strategies for regularizing the electromagnetic inverse scattering problem have been reported in the framework of the GNI method. These two strategies may be distinguished by the type of the cost-functional to be minimized. In the first strategy, the cost functional to be minimized is the data misfit functional $\mathcal{F}^{\mathcal{LS}}$ which is ill-posed [6], [9]–[14]. Due to this ill-posedness, we need to regularize (8) at each iteration of the GNI method. In the second strategy, the ill-posed nonlinear cost-functional $\mathcal{F}^{\mathcal{LS}}$ is first regularized and the GNI method is then applied to the regularized nonlinear cost-functional [3], [15]–[18]. Therefore, (8) does not need to be regularized throughout different GNI iterations. For every regularization method the regularization weight is either explicitly chosen or is implicit to the method. The basic idea behind the appropriate regularization weight for the GNI method is that the regularization weight should be high in early GNI iterations where the predicted solution is far from the true solution and should gradually decrease when the algorithm gets closer to the true solution. We refer to this idea as *adaptive* regularization [30], [31]. Throughout the paper, we denote the *positive* parameter α as the regularization parameter which (partially) governs the regularization weight. We now explain these two regularization strategies in more details.

A. The First Strategy

This strategy chooses the cost-functional to be minimized as the data misfit $\mathcal{F}^{\mathcal{LS}}$. Substituting (10) and (11) into (8), the GN correction at the n^{th} iteration is obtained by solving

$$\mathbf{J}_n \Delta\chi_n = d_n. \quad (12)$$

It is well-known that the matrix \mathbf{J}_n is an ill-conditioned matrix, making (12) a discrete ill-posed system of equations which needs to be regularized. There are two published general approaches for regularizing (12) in the electromagnetic inverse scattering case: penalty and projection methods.

1) *Penalty Methods*: Tikhonov regularization [32] is probably the most popular penalty method where the regularized solution of (12) is found from the minimization [9]–[13]

$$\Delta\chi_n = \arg \min_{\Delta\chi} \{ \|\mathbf{J}_n \Delta\chi - d_n\|^2 + \alpha_n \Omega(\Delta\chi) \}. \quad (13)$$

The regularization term $\Omega(\Delta\chi)$ is usually chosen to be in the form of an L_2 -norm, making (13) a least squares minimization. Herein, we assume $\Omega(\Delta\chi) = \|\mathbf{R}\Delta\chi\|^2$ where \mathbf{R} is an appropriate linear operator (matrix) whose nullspace intersects trivially with that of \mathbf{J}_n ; thus, ensuring a unique solution for (13). In this case, (13) can be written as a damped least squares minimization

$$\Delta\chi_n = \arg \min_{\Delta\chi} \left\| \begin{pmatrix} \mathbf{J}_n \\ \sqrt{\alpha_n} \mathbf{R} \end{pmatrix} \Delta\chi - \begin{pmatrix} d_n \\ \mathbf{0} \end{pmatrix} \right\|^2 \quad (14)$$

where $\mathbf{0}$ is the zero vector of appropriate size. The minimization (14) is equivalent to

$$\left(\mathbf{J}_n^H \mathbf{J}_n + \alpha_n \mathbf{R}^H \mathbf{R} \right) \Delta\chi_n = \mathbf{J}_n^H d_n. \quad (15)$$

In this case, the weight of the regularization is determined by the positive parameter α_n which needs to be chosen in each GNI iteration. This weight is usually determined using either the standard regularization parameter-choice methods [33] or some *ad hoc* techniques [10]–[13]. The standard regularization parameter-choice methods, such as the L -curve [34], [35] or the Generalized Cross-Validation (GCV) [12], [13], [36] methods, can be very computationally expensive and may also fail in choosing an appropriate regularization weight. For example, the GCV function may become very flat so that locating its minimum, which corresponds to an appropriate regularization parameter, will be numerically difficult [34].

The *ad hoc* techniques are usually faster but are dependent on the noise level of the measured data. Therefore, they may need to be modified for different microwave imaging systems. However, it is easier to incorporate the adaptive regularization to the *ad hoc* techniques as compared to the standard regularization parameter-choice methods. For example, in [11], the regularization parameter α_n is chosen to be proportional to $\|d_n\|^2$. That is, the regularization weight decreases during the GNI iterations; thus providing the adaptive regularization. It should also be mentioned that the penalty term $\Omega(\Delta\chi_n)$ can have other forms such as the L_1 -norm total variation or maximum entropy [18].

It should be mentioned that this type of regularization, when \mathbf{R} is chosen to be the identity matrix \mathbf{I} , may be viewed as the Levenberg-Marquardt approach [13], [26], [37] where the matrix $\mathbf{J}_n^H \mathbf{J}_n$ is augmented by $\alpha_n \mathbf{I}$.

2) *Projection Methods*: Projection methods attempt to regularize (12) by projecting it onto a subspace having a basis that can be used to represent the solution $\Delta\chi_n$ with sufficient accuracy while maintaining the stability. The projection may be achieved by Krylov subspace methods such as the conjugate

gradient least squares (CGLS) or least squares with QR factorization (LSQR) methods [6], [38]–[40]: at the k^{th} iteration of the Krylov subspace methods, the solution is restricted to lie in

$$\Delta\chi_n^{(k)} \in \mathcal{K}_k \left(\mathbf{J}_n^H \mathbf{J}_n, \mathbf{J}_n^H d_n \right) \quad (16)$$

where \mathcal{K}_k is the k -dimensional Krylov subspace defined by \mathbf{J}_n and d_n . The Krylov subspace algorithms, when applied to an ill-posed system of equations, exhibit a *semi-convergence* behavior [39], [41]. That is, they improve the solution at their early iterations, where the solution space is restricted to a Krylov subspace of small dimension, however, they start deteriorating the solution by inverting the noise in later iterations. Therefore, the stopping iteration k plays the role of the regularization parameter: the fewer the iterations, the stronger the regularization. The stopping iteration can be determined using either standard regularization parameter-choice methods such as the L -curve method [42] or by some *ad hoc* techniques [6], [40].

As in penalty methods, adaptive regularization is difficult to incorporate in the standard regularization parameter-choice methods whereas they can be easily incorporated into the *ad hoc* techniques. For example in [6], an *ad hoc* technique has been used to determine the regularization weight in the CGLS scheme: the stopping iteration of the CGLS regularization method was chosen to be 2 in early GNI iterations and then increased to 16 in later GNI iterations. Considering that the smaller the stopping iteration, the stronger the regularization, this *ad hoc* technique is an attempt at adaptive regularization for the GNI method.

The projection can also be achieved by the Truncated Singular Value Decomposition (TSVD) where the unknown $\Delta\chi_n$ is projected onto the subspace spanned by first few right singular vectors of the matrix \mathbf{J}_n [39], [43], [44]. Writing the Singular Value Decomposition (SVD) of the matrix \mathbf{J}_n as $\mathbf{J}_n = \mathbf{U}\mathbf{S}\mathbf{V}^H$, the regularized solution of (12) using the TSVD method can be written as

$$\Delta\chi_n = \sum_{i=1}^k \frac{u_i^H d_n}{s_i} v_i \quad (17)$$

where the left singular vector u_i and the right singular vector v_i are the i^{th} column of the orthonormal matrices \mathbf{U} and \mathbf{V} respectively. The singular value s_i is the i^{th} diagonal element of the matrix \mathbf{S} . In (17), the integer k , which determines the dimension of the subspace spanned by the right singular vectors v_i , is the regularization parameter: the smaller the k , the stronger the regularization. It should be mentioned that in (17), we have assumed that the singular values s_i are ordered in a non-increasing sequence; i.e., $s_i \geq s_{i+1} \geq 0$. Similar to Krylov subspace regularization methods, the regularization parameter k may be determined from standard regularization parameter-choice methods or *ad hoc* techniques.

Regarding the use of standard regularization parameter-choice methods such as the L -curve and GCV methods with the first regularization strategy, it should be noted that these methods are developed for linear inverse problems where the discrete Picard condition [45] is satisfied for the underlying

unperturbed problem [33], [46]. However, they may not be appropriate for nonlinear inverse scattering problems, especially when the initial guess to the GNI algorithm is very far from the true solution [13].

B. The Second Strategy

In the second strategy, the nonlinear ill-posed cost-functional $\mathcal{F}^{\mathcal{L}\mathcal{S}}$ is first regularized and then the GNI method is applied to the regularized cost-functional. Therefore, (8) does not need to be regularized throughout the GNI iterations. At least, three different methods for regularizing the cost-functional $\mathcal{F}^{\mathcal{L}\mathcal{S}}$ for the GNI method have been reported in the literature. These are additive, multiplicative and additive-multiplicative regularization.

1) *Additive Regularization*: In this case, $\mathcal{F}^{\mathcal{L}\mathcal{S}}$ is regularized by an additive term (see for example, [15], [17]):

$$\mathcal{F}(\chi) = \mathcal{F}^{\mathcal{L}\mathcal{S}}(\chi) + \alpha \mathcal{F}^{\mathcal{A}\mathcal{R}}(\chi) \quad (18)$$

where $\mathcal{F}^{\mathcal{A}\mathcal{R}}$ is an appropriate additive regularizer. The regularizer $\mathcal{F}^{\mathcal{A}\mathcal{R}}$ is usually chosen to be the L_2 -norm total variation of the contrast which may be written as

$$\mathcal{F}^{\mathcal{A}\mathcal{R}}(\chi) = \frac{1}{V} \int_{\mathcal{D}} |\nabla \chi(\mathbf{q})|^2 dv(\mathbf{q}) \quad (19)$$

where V is the volume (or area, in the case of tomographic configurations) of \mathcal{D} and ∇ denotes the spatial gradient operator. For this regularizer, it is straightforward to show

$$\partial \mathcal{F}^{\mathcal{A}\mathcal{R}} / \partial \chi^* = -\frac{1}{V} \nabla^2 \chi \quad (20)$$

$$\partial^2 \mathcal{F}^{\mathcal{A}\mathcal{R}} / \partial \chi^* \partial \chi = -\frac{1}{V} \nabla^2 \quad (21)$$

where ∇^2 denotes the Laplacian operator. Using this specific regularizer, the GN correction at the n^{th} iteration is found by solving

$$\left(\mathbf{J}_n^H \mathbf{J}_n - \gamma \boldsymbol{\Sigma} \right) \Delta \chi_n = \mathbf{J}_n^H d_n + \gamma \boldsymbol{\Sigma} \chi_n \quad (22)$$

where the matrix $\boldsymbol{\Sigma}$ is the discrete representation of the $(1/V)\nabla^2$ operator. The positive parameter γ is equal to $\alpha \mathcal{N}^{\mathcal{L}\mathcal{S}}$. In this case, the regularization weight is constant throughout different GNI iterations, as both the matrix $\boldsymbol{\Sigma}$ and its coefficient γ remain constant throughout different GNI iterations. Therefore, this regularization type will not provide adaptive regularization unless the user changes the regularization weight manually. In this case, the parameter α is usually chosen via *ad hoc* techniques [15], [17]. It should also be mentioned that this regularization method favors smooth solutions due to the presence of the matrix $\boldsymbol{\Sigma}$ in (22) which provides Laplacian regularization.

2) *Multiplicative Regularization*: In this case, the cost-functional $\mathcal{F}^{\mathcal{L}\mathcal{S}}$ is regularized with a multiplicative term ([3], [18])

$$\mathcal{F}_n(\chi) = \mathcal{F}^{\mathcal{L}\mathcal{S}}(\chi) \mathcal{F}_n^{\mathcal{M}\mathcal{R}}(\chi). \quad (23)$$

Herein, we consider the multiplicative regularizer $\mathcal{F}_n^{\mathcal{M}\mathcal{R}}$ as the weighted L_2 -norm total variation of the unknown contrast, defined as [3]

$$\mathcal{F}_n^{\mathcal{M}\mathcal{R}}(\chi) = \int_{\mathcal{D}} b_n^2(\mathbf{q}) \left(|\nabla \chi(\mathbf{q})|^2 + \alpha_n^2 \right) dv(\mathbf{q}) \quad (24)$$

where

$$b_n(\mathbf{q}) \triangleq V^{-\frac{1}{2}} \left(|\nabla \chi_n(\mathbf{q})|^2 + \alpha_n^2 \right)^{-\frac{1}{2}}. \quad (25)$$

The positive parameter α_n^2 is chosen to be $\mathcal{F}^{\mathcal{L}\mathcal{S}}(\chi_n) / \Delta V$ where ΔV is the volume (or area for the case of 2D inversion) of a single cell in the discretized domain \mathcal{D} . For the regularizer (24), it can be shown that

$$\partial \mathcal{F}_n^{\mathcal{M}\mathcal{R}} / \partial \chi^* = -\nabla \cdot (b_n^2 \nabla \chi) \quad (26)$$

$$\partial^2 \mathcal{F}_n^{\mathcal{M}\mathcal{R}} / \partial \chi^* \partial \chi = -\nabla \cdot (b_n^2 \nabla) \quad (27)$$

where $\nabla \cdot$ represents the divergence operator. Using this multiplicative regularizer, the Gauss-Newton correction can then be found by solving

$$\left(\mathbf{J}_n^H \mathbf{J}_n - \beta_n \mathcal{L}_n \right) \Delta \chi_n = \mathbf{J}_n^H d_n + \beta_n \mathcal{L}_n \chi_n \quad (28)$$

where \mathcal{L}_n represents the discrete form of the $\nabla \cdot (b_n^2 \nabla)$ operator and $\beta_n = \|d_n\|^2$. The operator \mathcal{L}_n , which changes throughout the GNI iterations, provides an edge-preserving regularization. That is, if one specific region of the reconstructed χ_n is homogeneous, the weight b_n^2 will be almost constant for that region. Therefore, the operator \mathcal{L}_n will be approximately equal to $b_n^2 \nabla^2$ which favors smooth solutions. On the other hand, if there is a discontinuity (edge) at some region of χ_n , the corresponding b_n^2 for that region will be small. Thus the discontinuity will not be smoothed out and will be preserved. A detailed explanation about the weighted Laplacian regularizer can be found in [47].

This multiplicative regularization *automatically* determines the regularization weight which is governed by the discrepancy between the measured data and the simulated data corresponding to χ_n . As can be seen from (28), the weight of the operator \mathcal{L}_n depends on $\|d_n\|^2$ which provides adaptive regularization. That is, if the predicted solution is far from the true solution, the regularization weight is high. When the predicted solution gets closer to the true solution, the L_2 -norm of the discrepancy d_n decreases; thus decreasing the regularization weight. Note that the multiplicative regularizer, $\mathcal{F}_n^{\mathcal{M}\mathcal{R}}$, can also be used with either the L_2 -norm [18] or the L_2 -norm total variation form [3]. As opposed to the weighted L_2 -norm total variation multiplicative regularizer, see (24), these two forms of

the multiplicative regularizer do not have the edge-preserving characteristic and will not be discussed in this paper.

3) *Additive-Multiplicative Regularization*: In this case, we regularize (2) as [16]

$$\mathcal{F}(\chi) = \mathcal{F}^{\mathcal{L}\mathcal{S}}(\chi) [1 + \alpha \mathcal{F}^{\mathcal{A}\mathcal{R}}(\chi)]. \quad (29)$$

Choosing $\mathcal{F}^{\mathcal{A}\mathcal{R}}$ as in (19), the GN correction can be found by solving

$$\left(\mathbf{J}_n^H \mathbf{J}_n - \lambda_n \boldsymbol{\Sigma} \right) \Delta \chi_n = \mathbf{J}_n^H d_n + \lambda_n \boldsymbol{\Sigma} \chi_n \quad (30)$$

where $\lambda_n = \alpha \|d_n\|^2 / [1 + \alpha \mathcal{F}^{\mathcal{A}\mathcal{R}}(\chi_n)]$. This regularization favors smooth solution due to the presence of the matrix $\boldsymbol{\Sigma}$ in (30). Unlike the additive regularization, see (22), the weight of the regularization is not constant but changes throughout the GNI iterations. As can be seen from (30), the regularization weight governed by the positive parameter λ_n decreases when the algorithm gets closer to the true solution. However, the user is still required to set the positive parameter α at the beginning of the GNI algorithm. The algorithm then provides adaptive regularization based on the given α . It should be pointed out that this regularization can be viewed as a multiplicative regularization when the regularizer is $1 + \alpha \mathcal{F}^{\mathcal{A}\mathcal{R}}(\chi)$ or as an additive regularization when the regularizer is $\mathcal{F}^{\mathcal{L}\mathcal{S}}(\chi) \mathcal{F}^{\mathcal{A}\mathcal{R}}(\chi)$.

V. CONSISTENT FRAMEWORK AND DISCUSSION

Considering that the contrast $\chi(\mathbf{q})$ is zero on the boundary of \mathcal{D} , it can be shown that the operators $\boldsymbol{\Sigma}$ and \mathbf{L}_n are self-adjoint and negative definite (see Appendix A for the proof). Therefore, the operators $\boldsymbol{\Sigma}$ and \mathbf{L}_n can be represented by $-\mathbf{A}^H \mathbf{A}$ and $-\mathbf{B}_n^H \mathbf{B}_n$ respectively (for example, using Cholesky decomposition [48, Section 4.2]). Using this notation, the GN correction in (22), (28) and (30) can be written respectively as

$$\left(\mathbf{J}_n^H \mathbf{J}_n + \gamma \mathbf{A}^H \mathbf{A} \right) \Delta \chi_n = \mathbf{J}_n^H d_n - \gamma \mathbf{A}^H \mathbf{A} \chi_n \quad (31)$$

$$\left(\mathbf{J}_n^H \mathbf{J}_n + \beta_n \mathbf{B}_n^H \mathbf{B}_n \right) \Delta \chi_n = \mathbf{J}_n^H d_n - \beta_n \mathbf{B}_n^H \mathbf{B}_n \chi_n \quad (32)$$

$$\left(\mathbf{J}_n^H \mathbf{J}_n + \lambda_n \mathbf{A}^H \mathbf{A} \right) \Delta \chi_n = \mathbf{J}_n^H d_n - \lambda_n \mathbf{A}^H \mathbf{A} \chi_n. \quad (33)$$

Now, if we consider $\Omega(\Delta \chi)$ in (13) as $\|\mathbf{R}(\Delta \chi + \chi_n)\|^2$, the GN correction corresponding to (13) can be written as

$$\Delta \chi_n = \arg \min_{\Delta \chi} \left\| \begin{pmatrix} \mathbf{J}_n \\ \sqrt{\alpha} \mathbf{R} \end{pmatrix} \Delta \chi - \begin{pmatrix} d_n \\ -\sqrt{\alpha} \mathbf{R} \chi_n \end{pmatrix} \right\|^2 \quad (34)$$

which is equivalent to solving

$$\left(\mathbf{J}_n^H \mathbf{J}_n + \alpha_n \mathbf{R}^H \mathbf{R} \right) \Delta \chi_n = \mathbf{J}_n^H d_n - \alpha_n \mathbf{R}^H \mathbf{R} \chi_n. \quad (35)$$

It can be easily seen that by choosing \mathbf{R} equal to \mathbf{A} , and α_n equal to either γ or λ_n , the penalty method applied to (12) is equivalent to the additive or additive-multiplicative regularization applied

to the data misfit $\mathcal{F}^{\mathcal{L}\mathcal{S}}$. Also, by varying \mathbf{R} throughout the GNI iterations and choosing it to be \mathbf{B}_n at the n^{th} GNI iteration and setting α_n equal to β_n , the penalty method applied to (12) will be equivalent to the multiplicative regularization applied to $\mathcal{F}^{\mathcal{L}\mathcal{S}}$.

It can be shown that Krylov subspace regularization provides similar results to TSVD regularization [49, p. 50], [39, p. 146] due to the similarity between the Krylov subspace basis and the SVD basis. It can also be shown that the effect of TSVD regularization is very similar to that of Tikhonov regularization when $\Omega(\Delta \chi) = \|\Delta \chi\|^2$ [49, p. 13], [33], [46]. Therefore, assuming appropriate regularization weight, Krylov subspace regularization and the TSVD regularization methods applied to (12) produce results which closely follow the Tikhonov solution

$$\Delta \chi_n = \arg \min_{\Delta \chi} \left\{ \|\mathbf{J}_n \Delta \chi - d_n\|^2 + \alpha_n \|\Delta \chi\|^2 \right\}. \quad (36)$$

Now, assuming $\Omega(\Delta \chi)$ in (13) to be $\|\mathbf{R}(\Delta \chi + \chi_n)\|^2$ and substituting $y = \mathbf{R}(\Delta \chi + \chi_n)$, the Tikhonov functional in (13) can be written as

$$y_n = \arg \min_y \left\{ \|\tilde{\mathbf{J}}_n y - \tilde{d}_n\|^2 + \alpha_n \|y\|^2 \right\} \quad (37)$$

where $\tilde{\mathbf{J}}_n = \mathbf{J}_n \mathbf{R}^{-1}$ and $\tilde{d}_n = d_n + \mathbf{J}_n \chi_n$. Note that, here, we have implicitly assumed that the inverse of the regularization matrix \mathbf{R} exists, which is not always true. Having found y_n from (37), the GN correction $\Delta \chi_n$ can be found by solving the well-posed system of equations

$$\mathbf{R} \Delta \chi_n = y_n - \mathbf{R} \chi_n. \quad (38)$$

Using the aforementioned similarity between the Tikhonov regularization and Krylov subspace regularization as well as the TSVD regularization, the regularized solution y_n obtained from (37) will be similar to the regularized solution obtained by applying Krylov subspace regularization or the TSVD method to

$$\tilde{\mathbf{J}}_n y_n = \tilde{d}_n. \quad (39)$$

Therefore, if we apply Krylov subspace regularization or the TSVD method to (39) to obtain y_n , and then find $\Delta \chi_n$ from (38), the resulting $\Delta \chi_n$ will be similar to the Tikhonov solution when $\Omega(\Delta \chi_n)$ is chosen to be $\|\mathbf{R}(\Delta \chi_n + \chi_n)\|^2$ which satisfies (35). Therefore, the TSVD and Krylov subspace regularization methods can be viewed in the same form as (31), (32), (33) and (35) by applying them to (39) rather than (12).

It should be noted that these regularization methods can all be applied from this framework and they will result in the same $\Delta \chi_n$ for the appropriate choice of the regularization operator and its weight. However, their application will differ in some important aspects such as the computational complexity. For example, although Krylov subspace regularization and TSVD methods, applied to (12), will result in similar solutions, the computational complexity of Krylov subspace regularization is significantly less than that of the TSVD method. A more

detailed computational complexity analysis of the regularization techniques considered herein can be found in Appendix B.

Among the regularization methods considered herein, the multiplicative and additive-multiplicative regularization methods *automatically* adjust the regularization weight and provide adaptive regularization throughout the GNI iterations. As opposed to other regularization methods considered herein, the multiplicative regularization *automatically* changes the regularization operator, \mathcal{L}_n , during the GNI iterations. This will result in an edge-preserving regularization if the multiplicative regularizer is chosen as the weighted L_2 -norm total variation of the unknown contrast.

VI. CONCLUSION

Different regularization methods in conjunction with the Gauss-Newton inversion method for electromagnetic inverse scattering problems were studied and classified into two categories. It was shown that all of these regularization methods can be viewed from within a single consistent framework after applying some modifications. This framework helps to clarify the function of these regularization and may lead to future advances.

APPENDIX A

SELF-ADJOINTNESS AND NEGATIVE DEFINITENESS

We here prove that the operators Σ and \mathcal{L}_n are self-adjoint and negative definite using a procedure similar to the standard approach for proving Green's first and second identities [50, p. 36]. Assume $\phi(\mathbf{q})$ and $\psi(\mathbf{q})$ are in a Hilbert space of complex functions defined over the bounded domain of interest \mathcal{D} with an inner product defined as

$$\langle \phi(\mathbf{q}), \psi(\mathbf{q}) \rangle_{\mathcal{D}} = \int_{\mathcal{D}} \phi^*(\mathbf{q}) \psi(\mathbf{q}) dv(\mathbf{q}). \quad (40)$$

Letting $b^2(\mathbf{q})$ be a positive function in this space, we may write,

$$\nabla \cdot (\phi^* b^2 \nabla \psi) = \phi^* \nabla \cdot (b^2 \nabla \psi) + \nabla \phi^* \cdot b^2 \nabla \psi \quad (41)$$

where the argument \mathbf{q} has been dropped for simplicity. Using the divergence theorem and definition of the inner product, we obtain

$$\langle \phi, \nabla \cdot (b^2 \nabla \psi) \rangle_{\mathcal{D}} + \int_{\mathcal{D}} b^2 \nabla \phi^* \cdot \nabla \psi dv(\mathbf{q}) = \oint_{\partial \mathcal{D}} b^2 \phi^* \frac{\partial \psi}{\partial n} da(\mathbf{q}) \quad (42)$$

where $\partial \mathcal{D}$ denotes the boundary of the domain of interest and $da(\mathbf{q})$ represents the differential area of $\partial \mathcal{D}$. The derivative $\partial/\partial n$ represents the outward directed normal derivative on the surface $\partial \mathcal{D}$. Interchanging ϕ^* and ψ and subtracting, we have

$$\begin{aligned} & \langle \phi, \nabla \cdot (b^2 \nabla \psi) \rangle_{\mathcal{D}} - \langle \nabla \cdot (b^2 \nabla \phi), \psi \rangle_{\mathcal{D}} \\ &= \oint_{\partial \mathcal{D}} b^2 \left(\phi^* \frac{\partial \psi}{\partial n} - \psi \frac{\partial \phi^*}{\partial n} \right) da(\mathbf{q}). \end{aligned} \quad (43)$$

Considering (43) and assuming ϕ and ψ vanish on $\partial \mathcal{D}$, it can be concluded that

$$\langle \phi, \nabla \cdot (b^2 \nabla \psi) \rangle_{\mathcal{D}} = \langle \nabla \cdot (b^2 \nabla \phi), \psi \rangle_{\mathcal{D}}. \quad (44)$$

The equality (44) implies that the operator $\mathcal{L} \triangleq \nabla \cdot (b^2 \nabla)$ is self-adjoint.

Letting $\phi = \psi$ in (42) and assuming that ϕ vanishes on $\partial \mathcal{D}$, we have

$$\langle \phi, \mathcal{L} \phi \rangle_{\mathcal{D}} = - \int_{\mathcal{D}} b^2 |\nabla \phi|^2 dv(\mathbf{q}) \quad (45)$$

Noting that the right hand side of (45) is negative, it can be concluded that the operator \mathcal{L} is negative definite. As the operator Σ is a special form of \mathcal{L} , when $b^2 = 1$, it is also self-adjoint and negative definite.

The assumption of vanishing ϕ and ψ on $\partial \mathcal{D}$ which was utilized to prove the self-adjointness and negative definiteness of the operators \mathcal{L} and Σ can be justified by noting that $\partial \mathcal{D}$ is outside the object being imaged. Thus, it is located in the background medium; meaning that the electric contrast is zero on $\partial \mathcal{D}$. Therefore, without loss of generality, we may redefine ϕ and ψ to be in a Hilbert space of complex functions defined over \mathcal{D} which vanish on $\partial \mathcal{D}$.

APPENDIX B

COMPUTATIONAL COMPLEXITY ANALYSIS

To compare the computational complexity of the regularization techniques considered in this paper, we utilize the following conventions: the number of transmitters is denoted by T_x and the number of receivers per transmitter by R_x . We further assume that the contrast function is discretized into an $N \times 1$ complex vector. Thus $\mathbf{J}_n \in \mathbb{C}^{R_x T_x \times N}$ and the calculation of both $\mathbf{J}_n r$ ($r \in \mathbb{C}^N$) and $\mathbf{J}_n^H s$ ($s \in \mathbb{C}^{R_x T_x}$) requires $R_x T_x N$ operations. The computational complexity of the CGLS and LSQR methods, as two Krylov subspace regularization schemes, is $2k \times (R_x T_x N)$ when applied to (12) (k is the dimension of the projection). Note that the CGLS and LSQR methods require two matrix-vector multiplications in each iteration. As k is usually chosen to be a very small integer, this regularization technique can be computationally attractive. The TSVD approach is computationally expensive as finding the SVD of the matrix \mathbf{J}_n in (12) requires $\mathcal{O}(R_x T_x N^2)$ operations if $R_x T_x \geq N$ or $\mathcal{O}(R_x^2 T_x^2 N)$ when $R_x T_x \leq N$ [42]. This can make the TSVD algorithm impractical for large-scale problems. It should also be noted that the TSVD method requires the explicit form of the matrix \mathbf{J}_n for performing the SVD. However, the other regularization methods discussed herein only require the definition of the matrix \mathbf{J}_n as a 'black-box' operator which implements two matrix vector multiplications: (i) $\mathbf{J}_n r$ and (ii) $\mathbf{J}_n^H s$. This can be very important in large-scale problems when the calculation of the explicit form of the Jacobian matrix is not feasible.

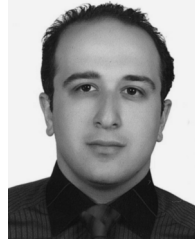
Comparing (15), (22), (28) and (30), it can be concluded that the computational complexity of the penalty methods and the methods which belong to the second strategy is very close.

The main difference between these methods lies in the computational cost of multiplying $\mathbf{R}^H \mathbf{R}$, $\mathbf{\Sigma}$ and \mathbf{L}_n by an arbitrary vector of the proper size. Specifically, the matrix $\mathbf{\Sigma}$ is a symmetric Block Toeplitz with Toeplitz Blocks [49, p. 100] and its matrix-vector multiplication can be accelerated by the Fast Fourier Transform (FFT). Therefore, the computational complexity of $\mathbf{\Sigma} \Delta \chi_n$ can be ignored compared to that of $\mathbf{J}_n^H \mathbf{J} \Delta \chi_n$. Using this approximation, the computational cost for finding the Gauss-Newton correction from (22) and (30) is about $2P \times (2R_x T_x N)$ operations where P is the number of conjugate gradient (CG) iterations required for convergence [assuming that the CG method is used for solving (22) and (30)]. Note that each iteration of the CG algorithm requires two matrix-vector multiplications and we have assumed that \mathbf{J}_n is only available as a 'black-box' operator. Therefore, it can be easily seen that the computational complexity of the Krylov subspace regularization applied to (12) is much less than that of the penalty methods as well as the methods of the second strategy due to the fact that usually $k \ll P$. However, it should be noted that the computational complexity of the Krylov subspace regularization techniques will increase drastically when applied to (39) as the operation of the matrices $\tilde{\mathbf{J}}_n$ and $\tilde{\mathbf{J}}_n^H$ on arbitrary vectors of correct size is expensive due to the presence of \mathbf{R}^{-1} in the definition of the matrix $\tilde{\mathbf{J}}_n$. If the methods of the first strategy utilize a standard regularization parameter-choice method, such as the L -curve algorithm or the GCV method, the computational cost of these algorithms needs to be considered in the overall computational cost of the regularization technique.

REFERENCES

- [1] M. Pastorino, S. Caorsi, and A. Massa, "A global optimization technique for microwave nondestructive evaluation," *IEEE Trans. Instrum. Meas.*, vol. 51, no. 4, pp. 666–673, Aug. 2002.
- [2] W. H. Weedon, W. C. Chew, and P. E. Mayes, "A step-frequency radar imaging system for microwave nondestructive evaluation," *Progr. Electromagn. Res.*, vol. 28, pp. 121–146, 2000.
- [3] A. Abubakar, T. M. Habashy, V. L. Druskin, L. Knizhnerman, and D. Alumbaugh, "2.5D forward and inverse modeling for interpreting low-frequency electromagnetic measurements," *Geophys.*, vol. 73, no. 4, pp. F165–F177, Jul.–Aug. 2008.
- [4] A. Abubakar and P. M. van den Berg, "Non-linear three-dimensional inversion of cross-well electrical measurements," *Geophys. Prospect.*, vol. 48, pp. 109–134, 2000.
- [5] L. P. Song, C. Yu, and Q. H. Liu, "Through-wall imaging (TWI) by radar: 2-D tomographic results and analyses," *IEEE Trans. Geosci. Remote Sensing*, vol. 43, no. 12, pp. 2793–2798, Dec. 2005.
- [6] T. Rubaek, P. M. Meaney, P. Meincke, and K. D. Paulsen, "Nonlinear microwave imaging for breast-cancer screening using Gauss-Newton's method and the CGLS inversion algorithm," *IEEE Trans. Antennas Propag.*, vol. 55, no. 8, pp. 2320–2331, Aug. 2007.
- [7] S. Y. Semenov, R. H. Svenson, A. E. Bulyshev, A. E. Souvorov, A. G. Nazarov, Y. E. Sizov, V. G. Posukh, A. Pavlovsky, P. N. Repin, A. N. Starostin, B. A. Voinov, M. Taran, G. P. Tastis, and V. Y. Baranov, "Three-dimensional microwave tomography: Initial experimental imaging of animals," *IEEE Trans. Biomed. Eng.*, vol. 49, no. 1, pp. 55–63, Jan. 2002.
- [8] A. Abubakar, P. M. van den Berg, and J. J. Mallorqui, "Imaging of biomedical data using a multiplicative regularized contrast source inversion method," *IEEE Trans. Microw. Theory Tech.*, vol. 50, no. 7, pp. 1761–1777, July 2002.
- [9] W. C. Chew and Y. M. Wang, "Reconstruction of two-dimensional permittivity distribution using the distorted Born iterative method," *IEEE Trans. Med. Imaging*, vol. 9, no. 2, pp. 218–225, 1990.
- [10] G. L. Wang, W. C. Chew, T. J. Cui, A. A. Aydinler, D. L. Wright, and D. V. Smith, "3D near-to-surface conductivity reconstruction by inversion of VETEM data using the distorted Born iterative method," *Inverse Problems*, vol. 20, pp. S195–S216, 2004.
- [11] N. Joachimowicz, C. Pichot, and J. P. Hugonin, "Inverse scattering: An iterative numerical method for electromagnetic imaging," *IEEE Trans. Antennas Propag.*, vol. 39, no. 12, pp. 1742–1752, Dec. 1991.
- [12] N. Joachimowicz, J. J. Mallorqui, J. C. Bolomey, and A. Broquetas, "Convergence and stability assessment of Newton-Kantorovich reconstruction algorithms for microwave tomography," *IEEE Trans. Med. Imag.*, vol. 17, pp. 562–569, Aug. 1998.
- [13] A. Franchois and C. Pichot, "Microwave imaging-Complex permittivity reconstruction with a Levenberg-Marquardt method," *IEEE Trans. Antennas Propag.*, vol. 45, no. 2, pp. 203–215, Feb. 1997.
- [14] A. E. Souvorov, A. E. Bulyshev, S. Y. Semenov, R. H. Svenson, A. G. Nazarov, Y. E. Sizov, and G. P. Tastis, "Microwave tomography: A two dimensional Newton iterative scheme," *IEEE Trans. Microw. Theory Tech.*, vol. 46, no. 11, pp. 1654–1659, Nov. 1998.
- [15] A. G. Tjihuis, K. Belkebir, and A. C. S. Litman, "Theoretical and computational aspects of 2-D inverse profiling," *IEEE Trans. Geosci. Remote Sensing*, vol. 39, no. 6, pp. 1316–1330, 2001.
- [16] J. D. Zaeytjd, A. Franchois, C. Eyraud, and J. Geffrin, "Full-wave three-dimensional microwave imaging with a regularized Gauss-Newton method-theory and experiment," *IEEE Trans. Antennas Propag.*, vol. 55, no. 11, pp. 3279–3292, Nov. 2007.
- [17] A. E. Bulyshev, A. E. Souvorov, S. Y. Semenov, R. H. Svenson, A. G. Nazarov, Y. E. Sizov, and G. P. Tastis, "Three dimensional microwave tomography. Theory and computer experiments in scalar approximation," *Inverse Problems*, vol. 16, pp. 863–875, 2000.
- [18] T. M. Habashy and A. Abubakar, "A general framework for constraint minimization for the inversion of electromagnetic measurements," *Progr. Electromagn. Res.*, vol. 46, pp. 265–312, 2004.
- [19] A. Franchois and A. G. Tjihuis, "A quasi-Newton reconstruction algorithm for a complex microwave imaging scanner environment," *Radio Sci.*, vol. 38, no. 2, 2003.
- [20] S. Barkeshli and R. G. Lautzenheiser, "An iterative method for inverse scattering problems based on an exact gradient search," *Radio Sci.*, vol. 29, pp. 1119–1130, 1994.
- [21] H. Harada, D. J. N. Wall, T. Takenaka, and M. Tanaka, "Conjugate gradient method applied to inverse scattering problem," *IEEE Trans. Antennas Propag.*, vol. 43, no. 8, pp. 784–792, Aug. 1995.
- [22] R. E. Kleinman and P. M. van den Berg, "A modified gradient method for two-dimensional problem in tomography," *J. Comput. Appl. Math.*, vol. 42, no. 1, pp. 17–35, 1992.
- [23] P. M. van den Berg and R. E. Kleinman, "A contrast source inversion method," *Inverse Problems*, vol. 13, no. 6, pp. 1607–1620, 1997.
- [24] S. Caorsi, A. Massa, and M. A. Pastorino, "A computational technique based on a real-coded genetic algorithm for microwave imaging purposes," *IEEE Trans. Geosci. Remote Sensing*, vol. 38, no. 4, pp. 1697–1708, 2000.
- [25] L. Garnero, A. Franchois, J. P. Hugonin, C. Pichot, and N. Joachimowicz, "Microwave imaging-complex permittivity reconstruction by simulated annealing," *IEEE Trans. Microw. Theory Tech.*, vol. 39, no. 11, pp. 1801–1807, Nov. 1991.
- [26] E. Chong and S. Zak, *An Introduction to Optimization*. New York: Wiley Interscience, 2001.
- [27] D. H. Brandwood, "A complex gradient operator and its application in adaptive array theory," *Proc. Inst. Elect. Eng.*, vol. 130, no. 1, pt. F and H, pp. 11–16, 1983.
- [28] A. van den Bos, "Complex gradient and Hessian," *Proc. Inst. Elect. Eng. Vision, Image Signal Process.*, vol. 141, no. 6, pp. 380–383, 1994.
- [29] P. R. McGillivray and D. W. Oldenburg, "Methods for calculating Fréchet derivatives and sensitivities for the nonlinear inverse problem: A comparative study," *Geophys. Prospect.*, vol. 38, pp. 499–524, 1990.
- [30] M. S. Zhdanov, *Geophys. Inverse Theory and Regularization*. Amsterdam, The Netherlands: Elsevier, 2002.
- [31] A. Abubakar and P. M. van den Berg, "Iterative forward and inverse algorithms based on domain integral equations for three-dimensional electric and magnetic objects," *J. Comput. Phys.*, vol. 195, pp. 236–262, 2004.
- [32] A. N. Tikhonov and V. Y. Arsenin, *Solutions of Ill-Posed Problems*. New York: Wiley, 1977.
- [33] P. C. Hansen, "Numerical tools for analysis and solution of Fredholm integral equations of the first kind," *Inverse Problems*, vol. 8, pp. 849–872, 1992.
- [34] P. C. Hansen and D. P. O'leary, "The use of the L-curve in the regularization of discrete ill-posed problems," *SIAM J. Sci. Comput.*, vol. 14, no. 6, pp. 1487–1503, Nov. 1993.
- [35] P. R. Johnston and R. M. Gulrajani, "Selecting the corner in the L-curve approach to Tikhonov regularization," *IEEE Trans. Biomed. Eng.*, vol. 47, no. 9, pp. 1293–1296, Sep. 2000.

- [36] G. H. Golub, M. Heath, and G. Wahba, "Generalized cross validation as a method for choosing a good ridge parameter," *Technometrics*, vol. 21, pp. 215–224, 1979.
- [37] A. Franchois, A. Joisel, C. Pichot, and J.-C. Bolomey, "Quantitative microwave imaging with a 2.45-GHz planar microwave camera," *IEEE Trans. Med. Imaging*, vol. 17, no. 4, pp. 550–561, Aug. 1998.
- [38] A. Bjork, *Numerical Methods for Least Squares Problems*. Philadelphia, PA: SIAM, 1996.
- [39] P. C. Hansen, *Rank-Deficient and Discrete Ill-posed Problems: Numerical Aspects of Linear Inversion*. Philadelphia, PA: SIAM, 1998.
- [40] J. D. Shea, P. Kosmas, S. C. Hagness, and B. D. van Veen, "Three-dimensional microwave breast imaging: A bounded, multi-frequency inverse scattering solution on a uniform voxel mesh," presented at the XXIX General Assembly of Int. Union of Radio Sci., Chicago, IL, Aug. 2008.
- [41] J. Chung, J. G. Nagy, and D. P. O'leary, "A weighted-GCV method for Lanczos-hybrid regularization," *Electron. Trans. Numer. Analysis*, vol. 28, pp. 149–167, 2008.
- [42] M. E. Kilmer and D. P. O'leary, "Choosing regularization parameters in iterative methods for ill-posed problems," *SIAM J. Matrix Anal. Appl.*, vol. 22, no. 4, pp. 1204–1221, 2001.
- [43] D. Colton and R. Kress, *Inverse Acoustic and Electromagnetic Scattering Theory*. New York: Springer-Verlag, 1992.
- [44] R. Pierri, A. Liseno, and F. Soldovieri, "Shape reconstruction from PO multifrequency scattered fields via the singular value decomposition approach," *IEEE Trans. Antennas Propag.*, vol. 49, no. 9, pp. 1333–1343, Sep. 2001.
- [45] P. C. Hansen, "The discrete Picard condition for discrete ill-posed problems," *BIT*, vol. 30, pp. 658–672, 1990.
- [46] P. C. Hansen, "Analysis of discrete ill-posed problems by means of the L-curve," *SIAM Review*, vol. 34, no. 4, pp. 561–580, Dec. 1992.
- [47] P. Charbonnier, L. Blanc-Féraud, G. Aubert, and M. Barlaud, "Deterministic edge-preserving regularization in computed imaging," *IEEE Trans. Image Processing*, vol. 6, no. 2, pp. 298–311, Feb. 1997.
- [48] G. H. Golub and C. F. V. Loan, *Matrix Computations*. Baltimore, MD: Johns Hopkins Univ. Press, 1996.
- [49] T. K. Jensen, "Stabilization Algorithms for Large-Scale Problems," Ph.D. dissertation, Tech. Univ. Denmark, Kongens Lyngby, Denmark, 2006.
- [50] J. D. Jackson, *Classical Electrodynamics*, 3rd ed. New York: Wiley, 1998.



Puyan Mojabi received the B.Sc. degree in electrical and computer engineering from the University of Tehran, Tehran, Iran, in 2002 and the M.Sc. degree in Electrical Engineering from Iran University of Science and Technology, Tehran, Iran, in 2004. Currently, he is working toward the Ph.D. degree in Electrical Engineering at the University of Manitoba, Winnipeg, MB, Canada.

His current research interests are computational electromagnetics and inverse problems.



Joe Lovetri (SM'09) received the Ph.D. degree in electrical engineering from the University of Ottawa, ON, Canada, in 1991.

From 1991 to 1999, he was an Associate Professor in the Department of Electrical and Computer Engineering, University of Western Ontario, Canada. He is currently a Professor in the Department of Electrical and Computer Engineering, and Associate Dean (Research) of the Faculty of Engineering at University of Manitoba, Winnipeg, Canada. His main research interests are in time-domain CEM,

modeling of EMC problems, GPR, and inverse problems.